Integrated microfluidic probe station

C. M. Perrault,[1,a)] M. A. Qasaimeh,[1,2] T. Brastaviceanu,[1] K. Anderson,[1] Y. Kabakibo,[1] and D. Juncker[1,2,3,b)]
[1]*Department of Biomedical Engineering, McGill University, Montréal, Quebec, H3A 1A4, Canada*
[2]*McGill University and Genome Quebec Innovation Centre, Montreal, Quebec, H3A 1A4, Canada*
[3]*Department of Neurology and Neurosurgery, McGill University, Montréal, Quebec, H3A 1A4, Canada*

(Received 5 March 2010; accepted 13 September 2010; published online 18 November 2010)

The microfluidic probe (MFP) consists of a flat, blunt tip with two apertures for the injection and reaspiration of a microjet into a solution—thus hydrodynamically confining the microjet—and is operated atop an inverted microscope that enables live imaging. By scanning across a surface, the microjet can be used for surface processing with the capability of both depositing and removing material; as it operates under immersed conditions, sensitive biological materials and living cells can be processed. During scanning, the MFP is kept immobile and centered over the objective of the inverted microscope, a few micrometers above a substrate that is displaced by moving the microscope stage and that is flushed continuously with the microjet. For consistent and reproducible surface processing, the gap between the MFP and the substrate, the MFP's alignment, the scanning speed, the injection and aspiration flow rates, and the image capture need all to be controlled and synchronized. Here, we present an automated MFP station that integrates all of these functionalities and automates the key operational parameters. A custom software program is used to control an independent motorized Z stage for adjusting the gap, a motorized microscope stage for scanning the substrate, up to 16 syringe pumps for injecting and aspirating fluids, and an inverted fluorescence microscope equipped with a charge-coupled device camera. The parallelism between the MFP and the substrate is adjusted using manual goniometer at the beginning of the experiment. The alignment of the injection and aspiration apertures along the scanning axis is performed using a newly designed MFP screw holder. We illustrate the integrated MFP station by the programmed, automated patterning of fluorescently labeled biotin on a streptavidin-coated surface. © *2010 American Institute of Physics.* [doi:10.1063/1.3497302]

I. INTRODUCTION

Microfluidic systems are being increasingly applied to biology and provide new advantages not available to traditional systems such as reduction of reagent consumption, control over the microenvironment, and parallelization. Microfluidic devices were for example used to pattern proteins or cells and to remove them selectively.[1–3] Generally, miniature, closed conduits are used to make microfluidic devices, although they entail many limitations. Different areas inside of the microchannel cannot be accessed readily as an open surface, high shear forces and flow resistance prevent rapid exchange of fluids, and in the particular case of working with cells, protocols for long term cell culture inside the channels often need to be developed before the cells can be used in the experiments of interest.[4]

Micropipettes are often used for the local delivery of reagents to arbitrary positions on a surface and to cells.[5–8] In most cases, a single pipette is used, and thus chemicals and liquid dispensed to a specific point diffuse to the surrounding areas. A push-pull setup was developed to counter this limitation and consists of either two concentric cannulae, where the inner cannula injects the reagent and the outer cannula aspirates it,[9–11] or of so-called theta pipettes where two barrels and their apertures are located side-by-side, symbolizing the Greek character θ.[12] However, such push-pull micropipettes lack consistency due to variability during fabrication, are fragile and break easily during operation because they are difficult to visualize, and require a high ratio of aspiration to injection flow rates for complete re-aspiration of the injected chemicals because of their configuration. Conversely, using sophisticated feedback controls, it is possible to use them for scanning across an inverted microscope in a setup similar to the one proposed here.[7,13]

The microfluidic probe (MFP) features two or more micrometer-scale apertures with a separation of a few tens of micrometers. The apertures are etched in a blunt tip, or mesa, a few hundred micrometers in diameter.[14–16] The MFP is mechanically robust and the blunt tip allows it to be positioned close to a substrate surface so as to form a micrometer-scale gap. A microjet injected into the gap is hydrodynamically confined with greater efficacy than with a micropipette because the mesa and substrate form a narrow gap that helps confine the injected microjet within the gap even for low ratios of aspiration to injection flow rate, Fig. 1. This configuration allows scanning of the MFP and the microjet across the surface with considerable speed while maintaining an efficient confinement of the microjet. The MFP

a)Present address: Institute of BioEngineering of Catalonia, 08028 Barcelona, Spain.
b)Electronic mail: david.juncker@mcgill.ca.

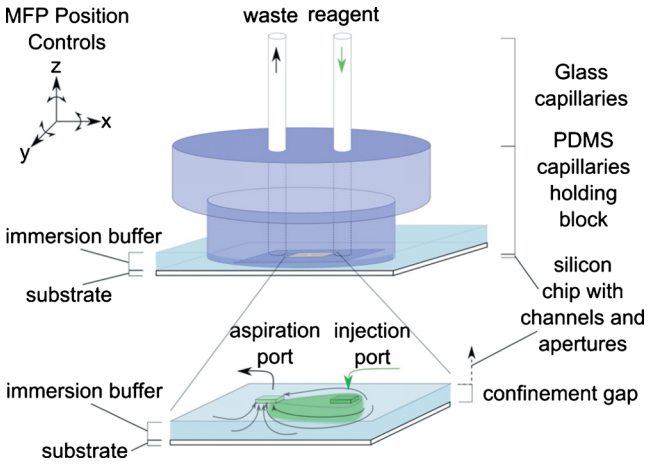

FIG. 1. (Color online) Schematic representation of the MFP head and the hydrodynamic confinement of a microjet (in green) between the blunt surface of the MFP and the substrate surface. The size of the confinement depends on the ratio of aspiration to injection flow rates, the size and separation of the apertures, and the gap. The MFP operation allows surface treatment in an immersed environment by flushing the confined stream across the surface.

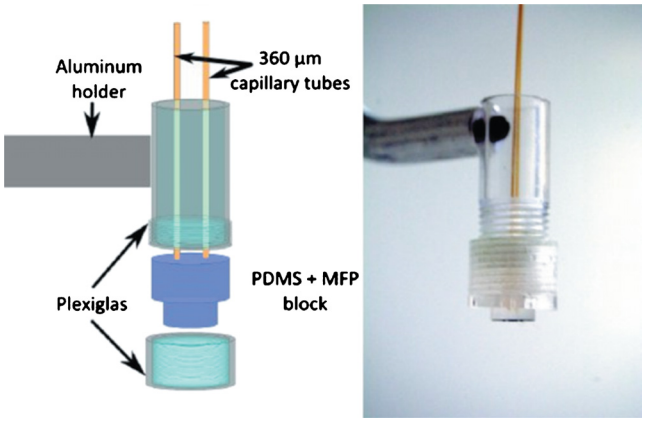

FIG. 2. (Color online) A custom-made MFP holder consisting of an aluminum handle and a PMMA screw-clamp. Clamping of the PDMS/MFP piece is performed by screwing the nut that also serves for rotational alignment of the MFP apertures along the X (or Y) axis. The Si chip with the mesa is bonded to the PDMS block. The two capillaries for injection and aspiration are plugged in from the top. The transparency of the Plexiglas allows the use of transmission illumination to visualize the probe and surface underneath when using low magnification objectives.

circumvents many of the constraints associated with closed microfluidic channels and can be used for random access microfluidics. The gap between the MFP and the surface, the scanning speed, and the injection and aspiration flow rates are critical parameters that need to be adjusted depending on the application. The use of the MFP hinges on the station used to control and manipulate it. For practical purposes, the control of all major parameters therefore needs to be integrated into a single user interface, and automated.

In this paper, we introduce a MFP station for operating the MFP that provides automated control over (i) the flow rate of the injection and aspiration streams, (ii) the microscope stage to adjust the XY position of the MFP on the substrate and an auxiliary Z stage to adjust the gap between the MFP and the bottom surface, (iii) the microscope to change objectives, filters, illumination, and so on, and that provides manual control over (iv) the horizontal alignment of the substrate surface to avoid out-of-plane drift when moving the stage, (v) the alignment of the injection and aspiration apertures along the X (or the Y) axis, and (vi) the parallel alignment between the MFP tip and the substrate surface to form a uniform gap with the substrate.

II. MATERIALS

A. Hardware setup

1. Microfluidic probe

The MFP consists of a microstructured tip made either in Si (Ref. 14) or in polydimethylsiloxane (PDMS),[16,17] in either case using microfabrication technologies. These tips comprise the microfluidic channels for injecting and aspirating different fluids.[18] For Si probes, an adaptor PDMS piece is bonded to the probe. The PDMS in all probes serves as the interface and is structured with receiving ports for inserting glass capillaries that are connected to the syringe pumps. Glass syringes (Hamilton, Reno, NV) with a volume between 1 and 500 μL are filled with filtered buffer solutions and connected to capillaries using nanotight fittings (Upchurch Scientific, USA) to minimize the dead volume. Air bubbles are avoided by degassing the solutions and filling the syringes through the back end before adding the piston. A buffer is flushed through the entire length of the capillaries, which are checked visually for any trapped bubbles under a microscope. The capillaries are then passed through the shaft of the holder prior to connection with the MFP head.[19]

To avoid trapping of air, the MFP head capillary ports are prefilled with buffer solutions using a plastic syringe prior to connection of the capillaries connected to the syringes. After the assembly, the probe head is clamped with the probe holder and mounted in the probe station.

2. Microfluidic probe holder

Different MFP holders have been used depending on the shape and make-up of the MFP.[14–17] Here we introduce a new design that comprises a lateral rod and a screw-clamp along with a matching PDMS interface chip. Figure 2 shows the different parts of the holder.

The handle was designed to be easily installed and removed from the positioning system, and made out of aluminum. Aluminum was chosen because of its low weight so as to avoid excessive stress on the goniometers. The MFP was made with a circular cross-section, allowing it to be clamped with a nut and screw, similar to a collet holder. First, the nut is taken off the threaded end of the holder head. The capillaries passing through the shaft of the head holder are connected to the MFP, and the nut is screwed back on the head, sandwiching the probe tightly. Plexiglas was used to make the clamp because it is transparent and thus permits use of the through-light illumination and the microscope's condenser. The screwing system allows easy rotation of the MFP around the Z-axis and its alignment along either the X- or Y-axis. The MFP holder is then attached to the positioning system and held in place with a fluted thumb screw. Instal-

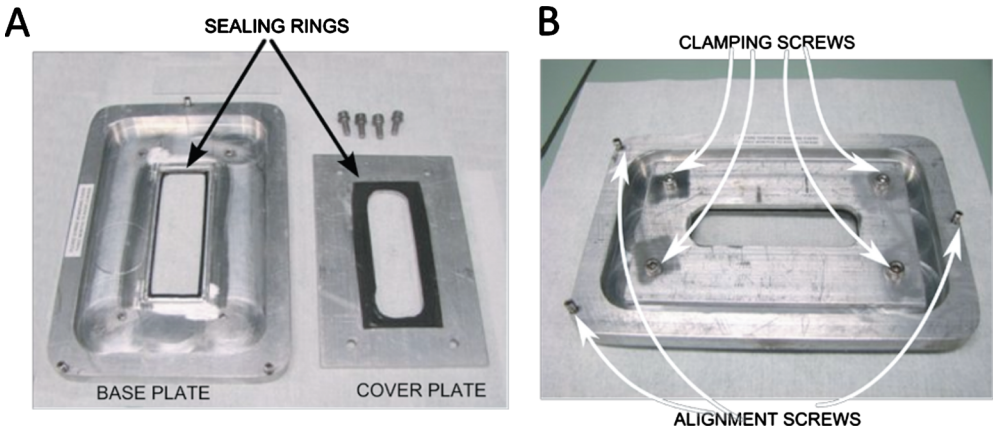

FIG. 3. (Color online) Custom slide insert with tilt adjustment mechanism. (a) Picture of the different elements of the slide insert including a base plate and a cover plate machined in Al with a central opening, sealing rings, and four screws for clamping a glass slide between the base and cover plates. (b) Picture of the assembled plates. Three set screws on the outer edges serve as support of the slide insert on the microscope stage and allow adjusting the horizontality of the slide. The alignment is critical because when scanning over long distances, a slight misalignment could alter the gap between MFP and substrate significantly.

lation and removal of the holder is simple and fast, allowing rapid switching between MFP operation and normal use of the microscope.

3. Slide insert

A customized slide insert for leak-tight clamping of standard 75×25 mm^2 rectangular glass slides was designed and machined in aluminum. A cover piece is screwed in place on top of the slide, and strips of waterproof foam cover the sides of the central opening, ensuring a tight impermeable seal around the glass slide and allowing immersed operation of the probe (Fig. 3). Three high-precision set screws [Fig. 3(b)], two located at the corners of one side and one at the center of the opposite side of the base plate, are used for leveling the slide insert with micrometer precision by iteratively focusing the image on the surface of the slide and adjusting the screws until the glass slide is perfectly horizontal and stays in focus while being scanned.

The gap between the probe head and the surface constrains the injected microjet in the vertical direction, and thus affects the rate and the shape of deposition. However, the specifications for common laboratory glass slides are loose, and for example the thickness can vary for up to 100 μm on a single slide. The set screws on the stage insert may be used to compensate for any linear thickness change, but if the slide surface is curved it cannot be compensated. Some slides have a curvature across the slide, and we observed waviness of the order of a few micrometers in height over a horizontal distance of a few millimeters. Given the relatively large diameter of the mesa and the four support posts of the probe head, it is not possible to compensate for variations taking place over short distances. For applications where the gap is <10 μm, one needs to evaluate the slide carefully to ensure that it is flat over the area of interest.

4. Microscopes

Two motorized inverted fluorescence microscopes (TE2000-E, Nikon), each outfitted with a rigid "wing" platform (Fig. 4) affixed with four screws on the main body of the microscope, have been transformed into MFP stations and are used for mounting the MFP. One of the systems is equipped with a confocal imaging system and as a result components from different vendors were used on each microscope, as described below. For imaging, we used either a cooled charge-coupled device (CCD) camera (Photometrics CoolSNAP HQ2, Tucson, AZ, USA) or an electron-multiplied CCD camera (Photometrics QuantEM:512SC) that can be switched between each microscope. The inverted microscope with the confocal system also includes a confocal spectral imaging setup (Nikon, C1si). Both microscopes are equipped with an X-Cite 120 illumination system (EXFO Photonics Solutions, Mississauga, Canada) and are mounted on vibration absorbing tables (TMC 63-534).

5. MFP positioning system

The positioning system of the MFP is used to adjust the XYZ position of the probe and its parallelism with the substrate. The MFP positioning system was specially made for the MFP and is shown in Figs. 4(a) and 4(b).

In the regular inverted microscope setup, the Z-axis positioning is performed using a high-resolution linear stage (LS-50 linear stage, Applied Scientific Instrumentation, Eugene, OR) outfitted with a glass ruler serving as a linear encoder and connected to the main stage controller with a serial RS232 interface (MS-2000 DC Servo motor control electronics, Applied Scientific Instrumentation, Eugene, OR). The stepper motor has a 20 nm step and the stage a precision of $\sim$100 nm, allowing for high accuracy positioning of the MFP above the substrate surface. X- and Y-axis controls are manual with two orthogonal linear stages and micrometer screws (M-443-4 and SM-50, Newport Corporation, Fountain Valley, CA) enabling a resolution below 1 μm. Typically, the MFP is positioned in the center of the field of view and stays there for the course of an experiment. The displacement of the MFP relative to the substrate during the experiment is effected by moving the XY stage of the microscope. The angle between the MFP head and the underlying surface is adjusted by rotating the rod and the MFP about

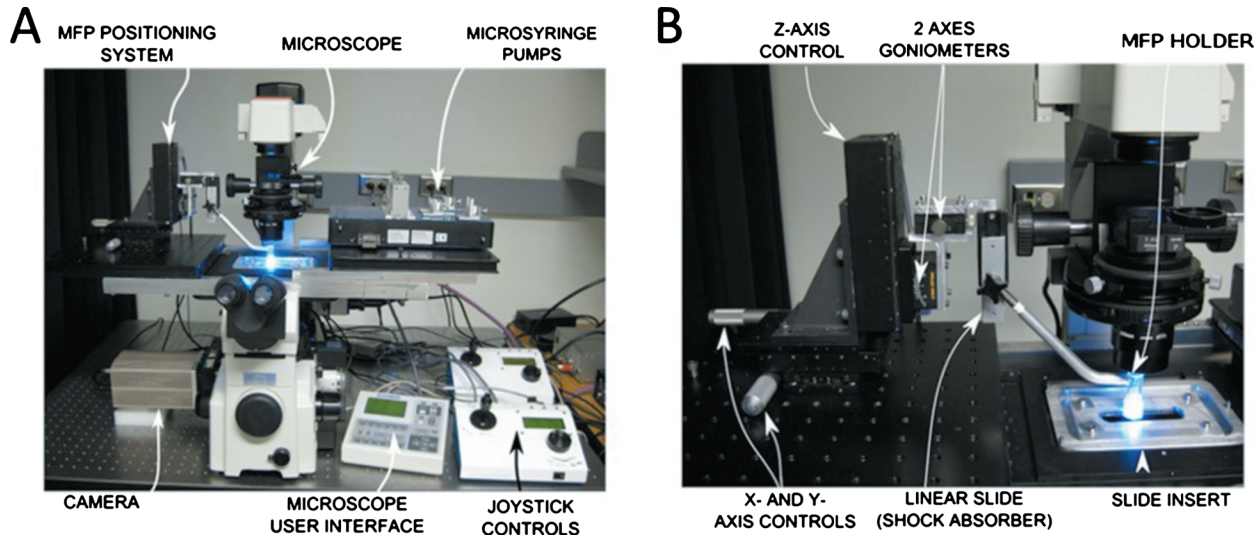

FIG. 4. (Color online) (a) Overview of the automated MFP station with its various components used for operating the MFP. The station integrates fluidic control using microsyringe pumps, positioning and movement control using the microscope stage, and imaging control using the CCD camera. The MFP positioning system is needed for accurate placement of the MFP over the surface. An environmental chamber was removed to allow visualizing the MFP positioning system. (b) Close-up view of the MFP positioning system. The assembly provides high-resolution x-, y-, and z-positioning of the MFP, as well as two-angle control using goniometers to ensure parallelism with the substrate. The linear motion slide acts as a shock absorber and support for the probe holder. The figure also shows the custom slide insert, MFP holder, and the illuminated MFP.

two axes using two manual goniometers (07GON503 and 07GON504, Melles Griot, Carlsbad, CA) each with a range of $\pm 20°$ and a resolution of 12 arc min. A freely moving linear stage (along the Z-axis) is attached to the goniometers and is part of the MFP holder. It serves as shock absorber in the event of contact between the MFP and the substrate, either during alignment or in the case of an unwanted crash, such as might be caused by human error or a software bug. For the microscope with confocal imaging, we used a motorized, computer controlled XYZ micromanipulator from Siskiyou (model 7600-XYZL, Siskiyou Inc, Oregon) to position the MFP.

Once installed in the positioning system, the MFP is aligned to the substrate to be processed with white light interference patterns that when observed between a lens and a flat surface give rise to the characteristic Newton's rings.[20] Using the inverted microscope, the blunt MFP head is monitored as it approaches the substrate. As the gap diminishes and becomes vanishingly small, interference fringes analogous to Newton's rings appear and form a stereotypical fringe pattern that originates at the point of contact of the MFP with the substrate. Using the goniometers, the angle between the probe and substrate is adjusted iteratively until only one ring appears over the entire MFP, providing direct submicrometer readout for the parallelism and for the gap between the MFP and the substrate, as shown in Fig. 5. The first fringe occurs for negative interference corresponding to a 180° phase change occurring for half a wavelength. The gap G for the first interference is thus $G=\lambda/2n$ with λ being the wavelength and n the refractive index, with $n=1$ for air and $n=1.33$ for water. Thus, assuming a wavelength $\lambda=500$ nm for the white light microscopy illumination, the first fringe will appear at 250 nm in air, and ~190 nm in water. Figure 5(d) shows the posts that are in contact whereas the central mesa is within the first interference fringe, which corresponds to a gap of ~190 nm and is likely due to a small curvature between MFP over the distance separating the posts. The apparition and disappearance of the interference fringes can be used to adjust the parallelism between the MFP and the substrate, and to reset the Z position of the controller to $z=0$ μm with very high accuracy.

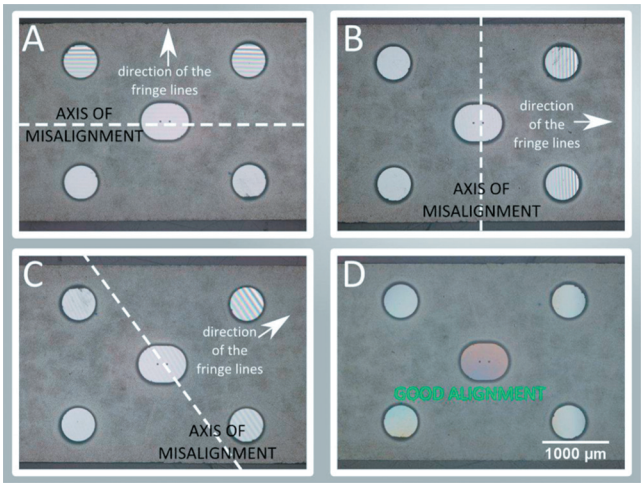

FIG. 5. (Color) The MFP is aligned using the white light interferences. The fringes observed originate at the point of contact between the MFP and the surface, and their width correlate with the parallelism of the MFP. (a)–(c) show misalignment of the MFP around various axes. The spacing between the fringe lines is indicative of the tilting angle of the MFP. Here, we can observe that the lines on the top right figure (b) are much closer than the lines on the top left (a) or bottom left (c) figures. This implies that the misalignment angle between the MFP head and the glass slide is greater on the top right figure than on the other two. (d) Shows a MFP parallel to the surface with a dark central mesa (first interference) and brighter posts. This result is due to a curvature between the MFP head and glass slide preventing contact of all features simultaneously. This setup allows alignment of the MFP with the substrate with submicrometer accuracy.

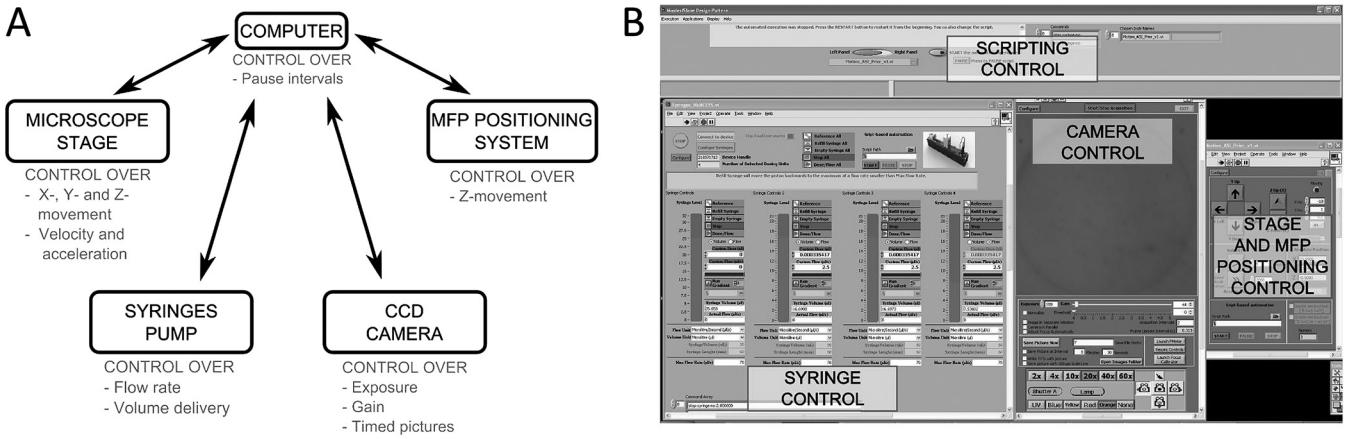

FIG. 6. (a) Simplified schematic of the Master-slave software architecture providing an overview of the computerized controls of the automated MFP station. (b) Screen capture of the LABVIEW software user interface. The software allows simultaneous control and monitoring of the syringe pumps, stage, camera, and microscope. Automated control of stage movement and dispensing can also be done using a script.

6. Microsyringe pumps

Microsyringes with volumes ranging between 1 and 500 μL are used and actuated using high precision syringe pumps that can be assembled as modules of up to 64 pumps (Nemesys, Cetoni, Germany). These pumps use linear motors with gear transmission and allow pulsation-free pumping over several hours with a single load, which translates into flow rates on the scale of femtoliters per second when using the smallest syringes.

7. Microscope stage

The inverted microscope setup includes a PZ-2000 microscope stage (Applied Scientific Instrumentation, Eugene, OR), featuring an XY stage with a high precision stepper motor (0.088 μm step and a typical <0.8 μm repeatability) and a piezoelement for Z control (range 100 μm, 1.5 nm resolution, and 1 nm repeatability, according to the manufacturer's specification). The confocal microscope is equipped with a Prior Scientific ProScan II stage with an XY axis resolution of 0.01 μm and a typical repeatability of <1 μm (Prior Scientific, Rockland, MA, USA).

8. Environmental chambers

For cell culture applications, it is essential to control the environmental conditions. Custom enclosures (Precision Plastics, Beltsville, MD) made of black Plexiglas were designed to accommodate the wing platform installed on each microscope, as described above. They offer control over humidity, temperature, and CO_2 levels while enabling fluorescence imaging experiments under daylight conditions for the operator.

B. Software

All components of the MFP system are controlled using software built with LABVIEW 8.5.1 (National Instruments, Austin, TX), designed with a modular architecture, Fig. 6(a). LABVIEW was chosen because it can be used to design intuitive user interfaces, which allows for modular readout and control of instruments, and permits subsequent modifications by future users.

LABVIEW virtual instruments were also readily available from Applied Scientific Instruments and Cetoni for operation of the linear stages and syringe pumps, respectively. There are no LABVIEW virtual instruments for the CCD cameras and Nikon Eclipse TE2000-E constituting a problem for the control of these equipments. This issue was resolved through the use of the open source MICRO-MANAGER package[21] and MATLAB. Although MICRO-MANAGER can interface with these devices (among many others), there is no direct way for LABVIEW to communicate with MICRO-MANAGER. Therefore, MATLAB (MathWorks Inc., Natick, MA) script nodes are used in the LABVIEW software, and MATLAB is used to issue commands through the MICRO-MANAGER application programming interface in order to acquire images from the camera and manipulate the microscope. However, as a consequence of this architecture, the imaging rate is reduced to 3 frames per second at most as compared to 15 frames per second when using the native camera software.

The LABVIEW software was programmed according to a master-slave architecture. The master interfaces with the user or can be driven by a script. The slaves are virtual instruments that run in parallel. There is no predefined set of (virtual) instruments; upon initialization, the user selects which instruments among microscope stage, probe holder, CCD camera, and syringe pumps need to be controlled depending on the needs of the particular experiment. Figure 6(b), is a screenshot showing a user interface with a control panel for the syringe pumps, the microscope, the camera and the microscope stage, as well as the scripting controls. Every set of instruments becomes an application instance, which can be configured and saved as a configuration file for future use. Moreover, the program is readily extensible because when a new device needs to be controlled, it can be added by programming a new virtual instrument from an existing template and added to the selection menu. The modular master-slave architecture gives the possibility to set execution priorities and to allocate computational resources for every individual module, and prioritize the time sensitive functions. In the case of the MFP, smooth displacement of the stage during surface patterning with the MFP is critical, but could not be achieved when the stage was controlled as part

of a loop with all the instruments because of delays due to other instruments. The stage control was thus prioritized and one of the two cores of the dual core microprocessor reserved for this task, which allowed overcoming this issue.

To automate surface patterning with the MFP, a scripting function was included in the software. The user is assisted in writing a script by selecting commands for every virtual instrument loaded for the application, and assigning values to their corresponding parameters. The commands appear in a list broken into sections for each instrument; they are written in natural language. No programming skills are needed for writing a script. Scripts are then saved as a text file, which can also be manually modified, and can be loaded from the main program to be run.

III. SURFACE PROCESSING WITH THE MFP

To illustrate the operation of the integrated MFP station, we demonstrate the preprogrammed patterning of a surface according to a script. Surface patterning of proteins had been shown previously,[1,9] but required a high concentration of proteins in both cases and special buffer conditions for the protein to successfully bind to the surface. Here, we introduce a new approach based on the high affinity binding between biotin and streptavidin. Biotin-streptavidin binding was chosen for MFP patterning, as it is (i) fast and benefits from the relatively high flow velocities under the probe, (ii) strong and thus withstands the shear forces of the flow, (iii) versatile since it can be used to immobilize many different proteins that are available in a biotinylated form, or that may be biotinylated before writing. A streptavidin coated slide (Xantec GmbH, Germany) was placed into the designed slide insert on top of the inverted microscope. An injection syringe with a capacity of 10 μL was loaded with phosphate buffer saline (PBS) containing 1 μg/ml biotinylated fluorescein (Sigma-Aldrich, St. Louis, MO, USA). A 100 μL aspirating syringe was filled with a small amount of PBS while monitoring and removing any trapped air, and while leaving ample volume for aspiration. Both syringes were connected to the MFP using a glass capillary and fittings. The injection and aspiration apertures of the MFP each featured a square cross-section with a 20 μm side length, were separated by 30 μm, and were located at the center of a mesa forming the blunt tip. Following careful alignment of the MFP parallel to the slide, PBS was added to the chamber, the MFP positioned 10 μm above the surface, and the aspiration started with a flow rate of 10 nL/s. The injection flow rate was set to 1 nL/s. During displacement, the microjet only flushes the surface briefly, and in addition, it is deflected and does not touch the surface when the substrate speed is sufficiently high.[14] When the stage is stopped, the microjet flushes the surface and binding between biotin and streptavidin results in a spot of fluorescent protein on the surface. Following a script created using the program's script writer, the stage velocity was set to 100 μm/s, and the MFP periodically immobilized for 2 s to form a series of spots following the binding of fluorescent biotin to the streptavidin slides, Fig. 7.

The deposition obtained with the MFP was compared to finite element modeling simulations performed using

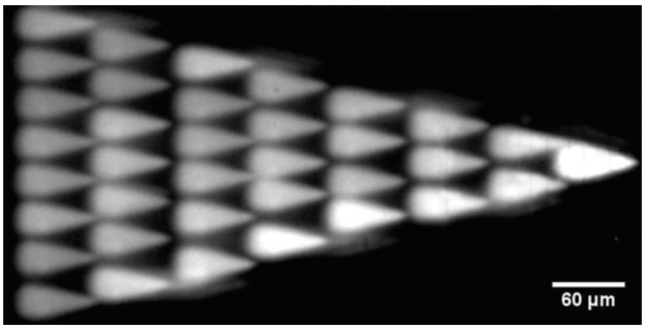

FIG. 7. Patterning of fluorescein-labeled biotin on a streptavidin-coated epoxy slide. The patterns were formed by rapidly moving the MFP from spot to spot, and using the injection and aspiration flow rate of 1 and 10 nL/s, respectively, a gap of 10 μm and a concentration of biotin of 1 μg/mL. The pattern was written from the bottom left side and moved up the first column, then right and down the second column and so forth. Vertical and horizontal displacement steps were 32 and 60 μm per step, respectively.

COMSOL MULTIPHYSICS 3.5 software with the same conditions as in the experiment. The flow profile predicted by the finite element simulation shown in Fig. 8 replicates that of the patterns obtained experimentally and shown in Fig. 7. The results shown are streaklines formed by massless particles injected into the gap and do not include diffusion that explains why the simulated pattern is smaller than the proteins deposited experimentally [as seen in Figs. 8(b) and 8(c)]. By virtue of the steady state conditions of the flow, streaklines correspond to streamlines in this case.[22]

In addition to ensuring precise spatial stability, the station provides repeatable positioning. Movement in the z-axis is controlled by a linear stage to which the MFP holder is attached. Recording the position of the MFP holder prior to large displacement up or down allows one to return to the same position afterwards. This was confirmed experimentally by verifying that the MFP returned to the image focus of a 40× objective. The accuracy of the xy stage that was

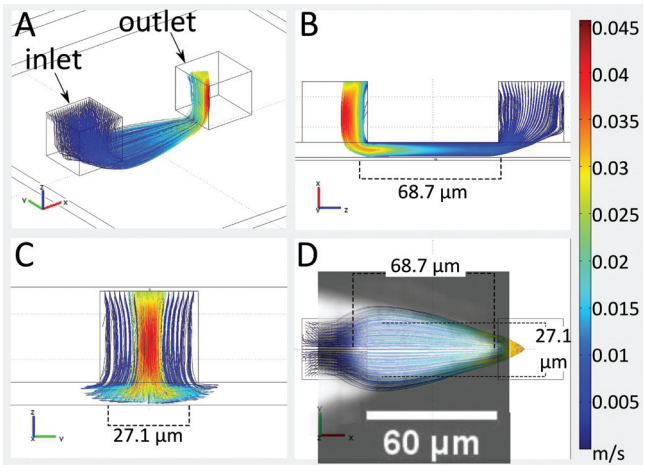

FIG. 8. (Color) Streaklines tracing simulations using finite-element analysis show the flow geometry of the reagents during operation of the MFP. (a) 3D view of the MFP and the flow. (b) and (c) Cross-sectional views along the xz and yz axes, respectively. (d) Superposition of top views of the experimental results (right most pattern from Fig. 7) and of the projection of the streakline patterns that both have similar shape. The length and width of the proteins deposited on the substrate are ~69 and ~27 μm respectively, and are reported in (c) and (d) for comparison.

outfitted with a linear glass ruler was beyond the measurement capability of the microscope. Using the probe station, it is thus possible to pause the patterning operation and move the probe and microscope slide, and later come back in the same position and complete the operation. The apertures of the probe used here are ~20 μm wide and are separated 40 μm center-to-center, resulting in patterns of 27 $\times$69 μm^2. The accuracy of the XY and Z stages is in the nanometer range, and was adequate for the vertical adjustment of the gap within less than one micrometer. This clearly exceeds the requirements needed for aligning these patterns. Smaller patterns may be achieved by reducing the size of the apertures, the gap, and the ratio of injection to aspiration, but because of the diffusive enlargement of the confined stream, sizes below 1 μm will be very difficult to achieve.[14] Hence, the probe station developed here will likely be adequate for most future developments and application of the microfluidic probe.

Deposition achieved with the MFP is controlled by the flow of the reagents, which is inhomogeneous across the substrate, and as a result, uniform deposition with this technique is a challenge. Fluid flowing along a line connecting the inlet and outlet ports flows at higher velocity than the fluid on the outer edge of the pattern. The higher the velocity, the shorter the residence time within the gap and the lower the chance for binding between streptavidin and biotin for each individual molecule, yet conversely, the chemicals are continuously replaced and no depletion occurs. On the outer edges of the tear drop shaped flow pattern, the residence time is longer, yet streaklines remain more distant from the substrate and diffusive flux is needed to transport the molecules to the surface. Overall, there are thus less molecules that reach the surface and less deposition occurs owing to lower mass transport and depletion of reagents. The velocity variation in the pattern also results in varying shear stress values. This may be expected to interfere with binding events for high values which would first occur close to the aspiration inlet where the shear stress is highest, although we did not observe it in the experiments we carried out. The configuration of the MFP thus makes uniform deposition challenging. Conversely, the concentration gradient formed during deposition is of interest for biomedical research and may be useful to study neuronal navigation for example.[23]

IV. CONCLUSION

The integrated MFP station presented here addresses the major requirements for setting up and automating the operation of the MFP by integrating the control of numerous equipments into one computerized platform. Computer control over the fluid flow, microscopy, and motion equipment allows for microfluidic surface processing based on keyboard or mouse commands given through the graphical user interface. Human manipulation errors are limited by automation, thereby greatly facilitating the operation of the MFP.

Several mechanical improvements were also presented. (i) A new MFP holder machined out of transparent plastic, allowing for overhead illumination. This holder also functions as the third goniometer and permits rotational alignment of the MFP during assembly. (ii) A slide holder with a three points support serving as an accurate tilting system for easy and fast alignment between the stage and glass slide to within 2–3 μm over the length of a slide, corresponding to 20 parts per million.

On the whole, the new setup provides the stability and control required for automated surface processing and generation of user-designed, customized patterns. The functionality of the station was illustrated by patterning of biotin onto streptavidin surfaces. Chemical deposition with the MFP uses minimal amounts of reagents; for example, the pattern in Fig. 7 was written in 80 s and consequently only required 80 nL of solution corresponding to 20 pg of biotin.

The MFP may be used to pattern cell guidance molecules as gradients on surfaces for cell chemotaxis studies, and further be used for locally perfusing cells growing on a substrate directly.[14] Alternatively, the MFP can be used for chemical surface patterning, such as by high precision resist removal.[15] The versatility of the MFP combined with the control capabilities of the station will allow its use by nonspecialist researchers who, instead on focusing on how to control and operate the MFP, may use it to address their particular research questions. Finally, thanks to the automation, much more complex patterns may be generated, in turn affording new research opportunities.

ACKNOWLEDGMENTS

The authors wish to acknowledge support from Canadian Foundation for Innovation (CF), Canada Institute for Health Research (CIHR) Regenerative and Nanomedicine grants, Natural Science and Engineering Research Council of Canada (NSERC), the McGill Nanotools Microfab Laboratory (funded by CFI, NSERC, and VRQ), and thank Matthieu Nannini and Nikolas Pekas for their help and advice, and Adiel Mallik for proof reading. M.A.Q. acknowledges the Alexander Graham Bell Canada Graduate NSERC Scholarship and D.J. acknowledges the Canada Research Chair.

[1] E. Delamarche, A. Bernard, H. Schmid, B. Michel, and H. Biebuyck, Science **276**, 779 (1997).
[2] S. Takayama, J. C. McDonald, E. Ostuni, M. N. Liang, P. J. A. Kenis, R. F. Ismagilov, and G. M. Whitesides, Proc. Natl. Acad. Sci. U.S.A. **96**, 5545 (1999).
[3] Y. C. Tung, Y. S. Torisawa, N. Futai, and S. Takayama, Lab Chip **7**, 1497 (2007).
[4] K. J. Regehr, M. Domenech, J. T. Koepsel, K. C. Carver, S. J. Ellison-Zelski, W. L. Murphy, L. A. Schuler, E. T. Alarid, and D. J. Beebe, Lab Chip **9**, 2132 (2009).
[5] P. B. Cook and F. S. Werblin, J. Neurosci. **14**, 3852 (1994).
[6] C. Y. Yue and Y. Yaari, J. Neurophysiol. **95**, 3480 (2006).
[7] L. Ying, A. Bruckbauer, D. Zhou, J. Gorelik, A. Shevchuk, M. Lab, Y. Korchev, and D. Klenerman, Phys. Chem. Chem. Phys. **7**, 2859 (2005).
[8] D. Klenerman and Y. Korchev, Nanomedicine **1**, 107 (2006).
[9] O. Feinerman and E. Moses, J. Neurosci. Methods **127**, 75 (2003).
[10] S. Kottegoda, I. Shaik, and S. A. Shippy, J. Neurosci. Methods **121**, 93 (2002).
[11] R. D. Myers, Physiol. Behav. **5**, 243 (1970).
[12] K. T. Rodolfa, A. Bruckbauer, D. Zhou, A. I. Schevchuk, Y. E. Korchev, and D. Klenerman, Nano Lett. **6**, 252 (2006).
[13] J. Gorelik, A. Shevchuk, M. Ramalho, M. Elliott, C. Lei, C. F. Higgins, M. J. Lab, D. Klenerman, N. Krauzewicz, and Y. Korchev, Proc. Natl. Acad. Sci. U.S.A. **99**, 16018 (2002).
[14] D. Juncker, H. Schmid, and E. Delamarche, Nature Mater. **4**, 622 (2005).

[15] R. D. Lovchik, U. Drechsler, and E. Delamarche, J. Micromech. Microeng. **19**, 115006 (2009).
[16] A. Queval, N. Ghattamaneni, C. Perrault, R. Gill, M. Mirzaei, R. McKinney, and D. Juncker, Lab Chip **10**, 326 (2010).
[17] M. A. Qasaimeh, R. Safavieh, and D. Juncker, presented at the MMB 2009, The Fifth International Conference on Microtechnologies in Medicine and Biology, Quebec, Canada, 2009.
[18] D. Juncker, H. Schmid, A. Bernard, I. Caelen, B. Michel, N. de Rooij, and E. Delamarche, J. Micromech. Microeng. **11**, 532 (2001).
[19] C. M. Perrault, M. A. Qasaimeh, and D. Juncker, J Vis Exp **28** (2009).
[20] J. Strong, *Procedures in Applied Optics* (Dekker, New York, 1989).
[21] N. Stuurman, N. Amdodaj, and R. Vale, Microscopy Today **15**, 42 (2007).
[22] F. M. White, *McGraw-Hill Series in Mechanical Engineering* (WCB/McGraw-Hill, Boston, MA, 1999), p. 106.
[23] A. C. von Philipsborn, S. Lang, J. r. Loeschinger, A. Bernard, C. David, D. Lehnert, F. Bonhoeffer, and M. Bastmeyer, Development **133**, 2487 (2006).